

Optical imaging of propagating Mach cones in water using refracto-vibrometry

Nathan R. Huber and Thomas M. Huber^{a)}

Department of Physics, Gustavus Adolphus College, 800 West College Avenue, St. Peter, Minnesota 56082, USA nhuber2@gustavus.edu, huber@gustavus.edu

Matthew T. Huber

Department of Physics, Rhodes College, 2000 North Parkway, Memphis, Tennessee 38112, USA hubmt-18@rhodes.edu

Abstract: Refracto-vibrometry was used to optically image propagating Mach cones in water. These Mach cones were produced by ultrasonic longitudinal and shear waves traveling through submerged 12.7 mm diameter metal cylinders. Full-field videos of the propagating wave fronts were obtained using refracto-vibrometry. A laser Doppler vibrometer, directed at a retroreflective surface, sampled time-varying water density at numerous scan points. Wave speeds were determined from the Mach cone apex angles; the measured longitudinal and shear wave speeds in steel $(6060 \pm 170 \, \text{m/s})$ and $3310 \pm 110 \, \text{m/s}$, respectively) and beryllium $(12\,400 \pm 700 \, \text{m/s})$ and $8100 \pm 500 \, \text{m/s})$ agreed with published values.

© 2017 Acoustical Society of America [DRD]

1. Introduction

Axisymmetric Mach cones are produced when the speed of a wave traveling through a submerged cylinder is faster than the speed of sound in water. Hydrophone arrays have been used to demonstrate Mach cone formation from submerged steel piles (roughly 0.75 m diameter hollow cylinders with a wall thickness of 25.4 mm) when they are driven into the ground for civil construction. These impulsive wave fronts are of concern for marine mammals and fish.

In the current study, full-field videos of Mach cones in water were obtained using an optical technique called refracto-vibrometry. Short ultrasonic impulses were incident on a 12.7 mm diameter cylinder submerged in a water tank. These impulses launched longitudinal and shear waves through the cylinder, resulting in the formation of Mach cones in the surrounding water. Non-invasive refracto-vibrometry measurements produced videos showing the formation and propagation of these Mach cones. The Mach cone apex angles were directly measured and analyzed to determine the longitudinal and shear wave speeds in steel and beryllium samples.

2. Theory: Mach cone formation

References 1 and 9 describe how a longitudinal wave traveling through a submerged cylindrical metal shell produces an axisymmetric Mach cone. The same basic mechanism applies to Mach cone formation from a solid metal cylinder. As the longitudinal waves travel through a cylinder at speed v_l , the Poisson effect induces a radial deflection of the surface. This radial deflection displaces a small amount of water. Because the longitudinal waves in the metal cylinder travel faster than the speed of sound in water, v_w , an axisymmetric Mach cone is formed with apex angle θ_l , such that

$$\sin \theta_l = v_w / v_l. \tag{1}$$

The longitudinal wave speed depends on the dimensions of the cylinder relative to the wavelength of the longitudinal waves. For the current experiment, where 2.25 MHz ultrasonic waves travel longitudinally in a steel cylinder, the wavelength is only a few millimeters. Because the wavelength is substantially smaller than the cylinder diameter, longitudinal waves travel at the same speed as in a bulk steel sample. For pile-driving, the longitudinal waves have frequencies² on the order of 1 kHz. This implies a

-

^{a)}Author to whom correspondence should be addressed.

wavelength of many meters, which is substantially larger than the pile's diameter and wall thickness. Theoretical models^{9,10} of wave propagation in thin-walled cylinders predict a reduction of the longitudinal wave speed relative to the speed in a bulk steel sample. This leads to a difference in the Mach cone apex angle from a solid steel cylinder in the current experiment compared to the thin-walled steel piles in Ref. 1.

As discussed in Sec. 4, a second Mach cone with a larger apex angle was observed in the current experiment. The Mach cone's apex angle was consistent with Eq. (1), except with the shear wave speed, v_s , replacing the longitudinal wave speed, v_l . These shear waves originate from the non-uniform force distribution when the ultrasonic focal spot is smaller than the diameter of the cylinder. This non-uniform force distribution imparts a shearing stress on the cylinder, launching shear waves. Shear waves were not noted in prior studies of impulsive driving of hollow cylindrical piles. ^{1,2} The wall thickness and diameter for steel piles were much smaller than the wavelength. This leads to a relatively uniform forcing distribution that reduces shear wave formation.

3. Experimental apparatus and methods

Refracto-vibrometry techniques were implemented as shown in Fig. 1. For an array of scan points, the measurement beam of a Polytec PSV-400-M2-20 scanning laser Doppler vibrometer (Polytech GmbH, Waldbronn, Germany) was directed through a water tank toward a retro-reflective surface. To optically detect the passage of ultrasonic wave fronts, the vibrometer monitored the phase difference between the measurement beam and an internal reference. Density fluctuations of a wave front in water have a corresponding change in index of refraction. As the retro-reflected measurement beam traversed the water tank, it accumulated a total phase shift based on the integrated index of refraction (called the optical path length⁶). When an ultrasonic wave front passed through the measurement beam, the vibrometer converted the resulting time-varying phase shifts into a time-varying voltage. The refracto-vibrometry technique is most sensitive to density variations in regions where the measurement beam is perpendicular to the direction of travel of a wave front;⁴ this yields a single slice of the Mach cone. By sequentially measuring a large number of scan points, a full-field dataset of propagating wave fronts was obtained.

Ultrasonic impulses from a Panametrics V305 2.25 MHz transducer (Olympus NDT, Waltham, MA) were directed toward the face of a solid metal cylinder. The transducer and cylinder were separated in the water tank by the transducer's 37 mm focal length. In independent trials, 12.7 mm diameter steel and beryllium cylinders were used. The water temperature of 21 ± 1 °C implies a speed of sound of $v_w = 1486 \pm 3$ m/s.

The vibrometer measurement head was mounted 1.5 m from the water tank. The angle of incidence on the glass surface never exceeded 5°, thus Snell's law corrections were negligible. The vibrometer's 20 MHz bandwidth DD-300 displacement decoder output was sampled at 51 MHz. To reduce noise, 200 separate ultrasound pulses were time averaged for each scan point. In post processing, a sliding average of six sequential samples led to an effective down-sampled rate of 8.5 MHz. An array of about 30 000 scan points was measured for each metal cylinder.

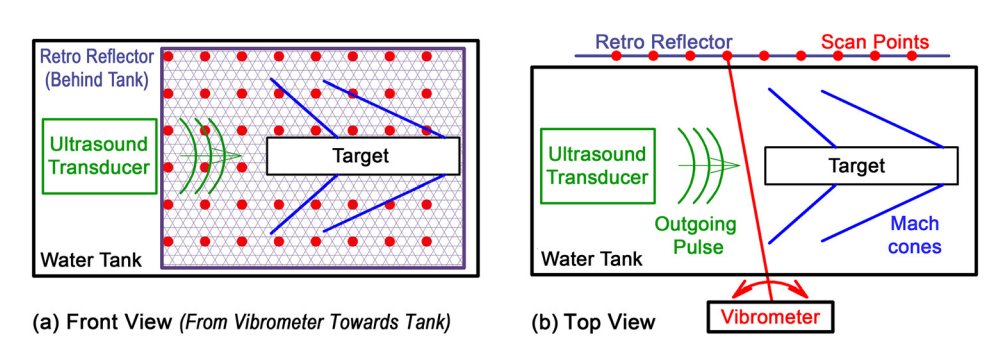


Fig. 1. (Color online) Experimental apparatus (a) front view and (b) top view. The pulse from an ultrasound transducer passes through water where it is focused onto a cylindrical metal target. To measure propagating wave fronts using refracto-vibrometery, the laser measurement beam emitted from a scanning laser Doppler vibrometer passes through a water tank, is reflected from a retro-reflective surface, and returns to the vibrometer head.

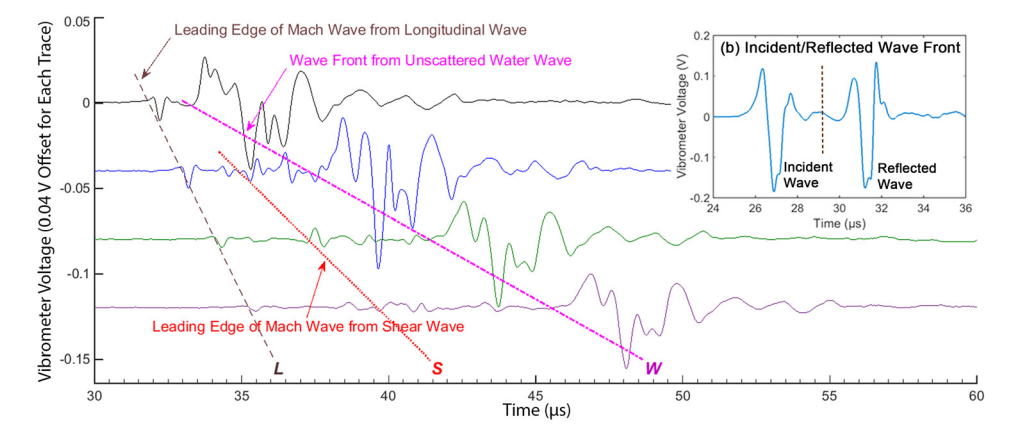


Fig. 2. (Color online) Refracto-vibrometry measurements for four scan points parallel to the axis of the metal cylinder. The lines L and S indicate Mach cones due to longitudinal and shear waves. The line W indicates wave fronts from unscattered ultrasonic waves. Inset graph (b) is from a scan point showing the incident and reflected wave fronts on the cylinder face.

4. Results

With the refracto-vibrometry technique, each scan point yielded a time-varying voltage related to density variations as waves passed through the measurement beam. Figure 2 shows wave forms from four scan points, parallel to the axis of the cylinder and roughly 6.6 mm apart. To aid visualization, each successive trace is offset vertically by $0.04\,\mathrm{V}$. A portion of the incident ultrasound impulse does not impact the cylinder, but travels unscattered through the tank at $1486\,\mathrm{m/s}$. The leading edge of this unscattered ultrasonic wave is indicated by the line W in Fig. 2. The Mach cone produced from longitudinal waves traveling through the cylinder leads to impulses arriving earlier than the unscattered wave. The dashed line L shows the first arrival of this Mach cone. The dotted line S shows the first arrival of a separate shear-wave produced Mach cone. While clearly visible in Fig. 3, the arrival of this shear-wave produced Mach cone is difficult to discern in the small collection of scan points in Fig. 2.

Mm. 1 and Mm. 2 are videos of the full set of superimposed scan points. They clearly show the incoming wave front and the emergence of the Mach cones produced by longitudinal and shear waves. Figures 3(a) and 3(b), extracted from a single frame of Mm. 1, show the wave fronts emitted by steel and beryllium cylinders. Beryllium has wave speeds over twice that of steel, so the Mach cones from the beryllium cylinder have much smaller apex angles than the steel cylinder. In Fig. 3, the lines denoted W, L, and S are defined as in Fig. 2: the leading edge of the unscattered wave, and the Mach cones produced by the longitudinal and shear waves.

Mm. 1. Refracto-vibrometry video of propagating Mach cones in water after ultrasonic pulse excitation of steel and beryllium cylinders. Negative vibrometer voltages, corresponding to negative density variations, are scaled to darker blue shading. This file is of type "mp4" (7.2 MB).

Mm. 2. Refracto-vibrometry video of propagating Mach cones in water after ultrasonic pulse excitation of steel and beryllium cylinder. Positive and negative vibrometer voltages are scaled to green and red, respectively. This file is of type "mp4" (7.4 MB).

The apex angles in Mm. 1 were used to determine the longitudinal and shear wave speeds for the steel and beryllium samples. The Mach cone angles were manually measured for multiple frames using an on-screen tool. For the steel cylinder, the Mach

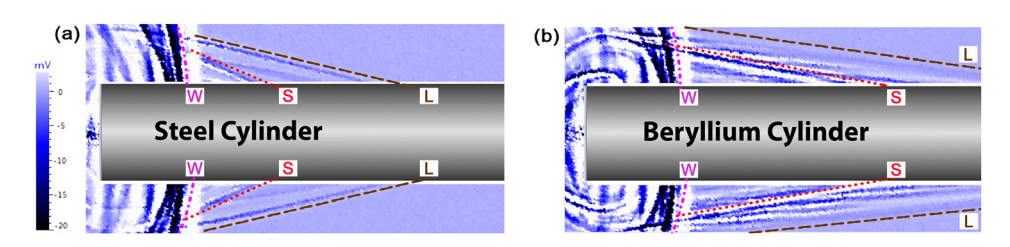


Fig. 3. (Color online) Refracto-vibrometry measurements of Mach cones for (a) steel and (b) beryllium cylinders in water. These images are extracted from a single frame of the video Mm 1. The lines L and S indicate Mach cones due to longitudinal and shear waves. The line W indicates wave fronts from unscattered ultrasonic waves.

cone produced by the longitudinal wave had an average apex angle of $\theta_I = 14.2 \pm 0.4^{\circ}$. The shear-wave produced Mach cone had an apex angle of $\theta_s = 26.7 \pm 1.0^{\circ}$; the larger uncertainty was due to distortions from interfering Mach cones. Using Eq. (1), the resulting longitudinal and shear wave speeds in the steel sample were 6060 ± 170 and 3310 ± 110 m/s, respectively. These are in good agreement with published values of 5960 and 3235 m/s. Similarly, for the beryllium sample, the Mach cone angles from the longitudinal and shear waves were $6.9 \pm 0.4^{\circ}$ and $10.6 \pm 0.6^{\circ}$. The resulting longitudinal and shear wave speeds in the beryllium sample, 12400 ± 700 and 8100 ± 500 m/s, were consistent with published values of 12890 and 8880 m/s.

5. Conclusions

The results clearly illustrate the efficacy of using refracto-vibrometry to obtain full-field videos of propagating Mach cones. In this study, the Mach cones were produced by ultrasonic longitudinal and shear waves traveling in steel and beryllium cylinders. The wave speeds, measured using the Mach cone apex angles, were in good agreement with published speeds.

A future study will investigate whether refracto-vibrometry can be used for quantitative investigation of Mach cones produced using alternate cylinder geometries. For example, longer-wavelength ultrasound transducers could be used with small-diameter, thin-walled cylinders. By making the ultrasonic wavelength larger than the sample dimensions, the study may better model Mach cone production by impact-driven steel piles.

Acknowledgments

The authors would like to thank Brent Hoffmeister of Rhodes College Physics Department for loaning equipment and valuable discussions. This material is based upon work supported by the National Science Foundation under Grant Nos. 1300591 and 1635456.

References and links

- ¹P. G. Reinhall and P. H. Dahl, "Underwater Mach wave radiation from impact pile driving: Theory and observation," J. Acoust. Soc. Am. **130**(3), 1209–1216 (2011).
- ²P. H. Dahl and P. G. Reinhall, "Beam forming of the underwater sound field from impact pile driving," J. Acoust. Soc. Am. **134**(1), EL1–EL6 (2013).
- ³P. H. Dahl, C. A. F. de Jong, and A. N. Popper, "The underwater sound field from impact pile driving and its potential effects on marine life," Acoust. Today 11(2), 18–25 (2015).
- ⁴A. R. Harland, J. N. Petzing, and J. R. Tyrer, "Nonperturbing measurements of spatially distributed underwater acoustic fields using a scanning laser Doppler vibrometer," J. Acoust. Soc. Am. 115(1), 187–195 (2004).
- ⁵E. Olsson and K. Tatar, "Sound field determination and projection effects using laser vibrometry," Meas. Sci. Technol. 17(10), 2843–2851 (2006).
- ⁶R. Malkin, T. Todd, and D. Robert, "A simple method for quantitative imaging of 2D acoustic fields using refracto-vibrometry," J. Sound Vib. 333(19), 4473–4482 (2014).
- ⁷N. Kudo, "A simple technique for visualizing ultrasound fields without Schlieren optics," Ultrasound Med. Biol. **41**(7), 2071–2081 (2015).
- ⁸M. T. Huber, N. Huber, and T. Huber, "Optical detection of Mach shock wave cones in water using refracto-vibrometry," J. Acoust. Soc. Am. 140(4), 3410–3410 (2016).
- ⁹M. V. Hall, "An analytical model for the underwater sound pressure waveforms radiated when an off-shore pile is driven," J. Acoust. Soc. Am. 138(2), 795–806 (2015).
- ¹⁰M. C. Junger and D. Feit, Sound, Structures, and Their Interaction (MIT Press, Cambridge, MA, 1986).
- ¹¹W. M. Haynes, CRC Handbook of Chemistry and Physics, 96th ed. (CRC Press, Boca Raton, FL, 2015).
- ¹²W. Wilson, "Speed of sound in distilled water as a function of temperature and pressure," J. Acoust. Soc. Am. 31(8), 1067–1072 (1959).